

**Supporting Information for the manuscript ‘Atomic-scale electron-beam
sculpting of near-defect-free graphene nanostructures’**

*Bo Song, Grégory F. Schneider, Qiang Xu, Grégory Pandraud, Cees Dekker,
Henny Zandbergen**

Content

- Heating holder that was used
- Sample preparation
- Parameters for TEM sculpting and imaging
- Contamination
- Fourier transforms of images in Figure 1
- Recrystallization at $T > 500$ °C after amorphization at room temperature
- Straight cylindrical nanopores
- Sculpting strategy
- Carbon nanotubes
- Polycrystalline graphene nanoribbons at 500 °C
- Prospective: More efficient sculpting of graphene by better hardware
- List of movies supplied

to whom the correspondence should be addressed, h.w.zandbergen@tudelft.nl

Heating holder with MEMS heater used for in-situ experiments

For the in-situ experiments, a SiN membrane was used with an embedded, coiled Pt wire, see also Fig.S1 [S1]. In the SiN membrane, a 5 μm diameter hole was made with a focussed ion beam in between the windings of the Pt wire to allow substrate-free TEM imaging of the graphene. The very low heat capacity of the heater results in low thermal drift, which enables stable high-resolution electron microscopy at elevated temperature. We were able to take images with exposure times up to 10 seconds without loss of atomic resolution due to specimen drift. The temperature of the sample is determined by from the resistance of the Pt heater, using a calibration of such heaters with a furnace and calibrated thermocouple.

Sample preparation

Graphene flakes were prepared by exfoliation of natural graphite (NGS graphite) on a 285 nm thermally grown SiO₂/Si wafer (Nova electronic materials). Graphene flakes of interest were selected using optical interference microscopy (Fig.S1a) [S2]. Such a graphene flake was then transferred on top of the hole in SiN membrane (see previous section) using the wedging transfer technique [S3] (Fig. 1b). For this, first, a hydrophobic polymer (cellulose acetate butyrate dissolved in ethyl acetate, 30 mg/mL) was deposited on the Si-SiO₂-graphene ensemble. Subsequently this polymer coating with the graphene moulded into it was wedged at the air/water interface, yielding a floating film at the air/water interface. Next, the MEMS microheater was positioned under the film, and brought into contact with graphene by lowering the level of the water. Submicron positioning was carried using micromanipulators. Finally the polymer was dissolved in pure ethyl acetate.

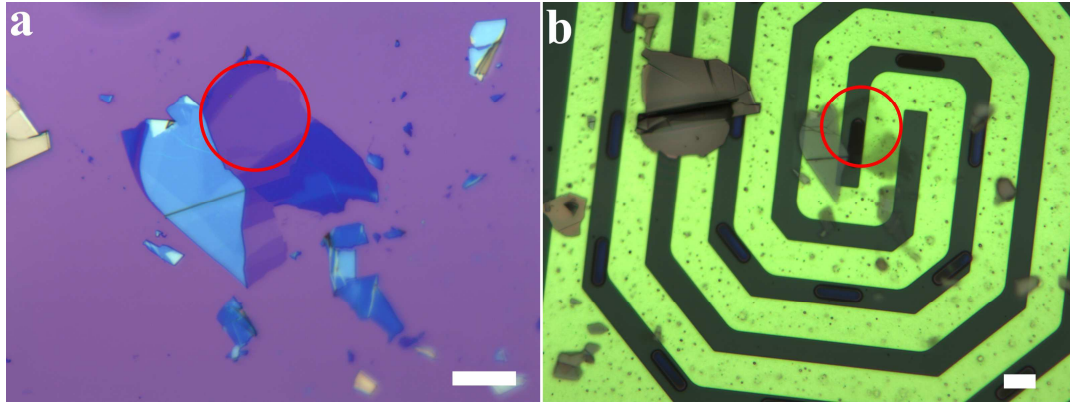


Figure S1. Transfer of graphene to a MEMS heater. (a) Optical image of graphene flakes on a SiO₂-coated Si wafer. (b) Optical image of the same graphene flake (marked by red circle) after transfer on top of the hole on the Pt microheater. Scale bars: 10 μ m.

Parameters for TEM sculpting and imaging

The TEM imaging was performed in a cubed FEI Titan microscope with a post-specimen corrector. The spherical aberration is always corrected to below 1 micron. The entire experiment was conducted in the high vacuum environment (10^{-8} ~ 10^{-7} torr) of the microscope chamber. The typical electron beam current during the imaging at 300 kV is 10^5 electrons/nm²s. Because of the low drift of our MEMS heating holder, we were able to use a long exposure time (typically six seconds) to make single-shot images on a 2K by 2K Gatan CCD camera. Image sequences from the movies are performed with a typical interval time of 12 seconds. Then these image sequences are manually aligned and converted into movies via software Image J (Rasband, W.S., *ImageJ*, U. S. National Institutes of Health, Bethesda, Maryland, USA, <http://rsb.info.nih.gov/ij/>).

Contamination

The rate of contamination is measured by putting a 20 nm diameter electron beam of the transmission electron microscope operated at 300 kV on the graphene sample and subsequent monitoring of the increase of amorphous carbon deposition in time. When this contamination test is done at room temperature, a fast carbon deposition can be observed (Figure S2). Continuation of this electron beam irradiation leads to a continuous growth of the contamination. This contamination phenomenon is due to the continuous surface diffusion of hydrocarbons to the electron beam area, where those molecules are cracked to carbon. If the sample is pre-heated at 400°C for several minutes, however, the fast continuous growth of contamination is no longer observed at RT, although still some amorphous material is observed in the electron beam area. After preheating at 400°C but over overnight storage of the specimen at room temperature in the TEM, the build-up of contamination is again much faster and continuous. Pore drilling at room temperature is very slow as can be seen from Fig. S2 - point 3, where hardly any difference with its surrounding can be seen. Pore drilling it is faster at 500°C than at 200° C (see points 4 and 5 in Fig. S2).

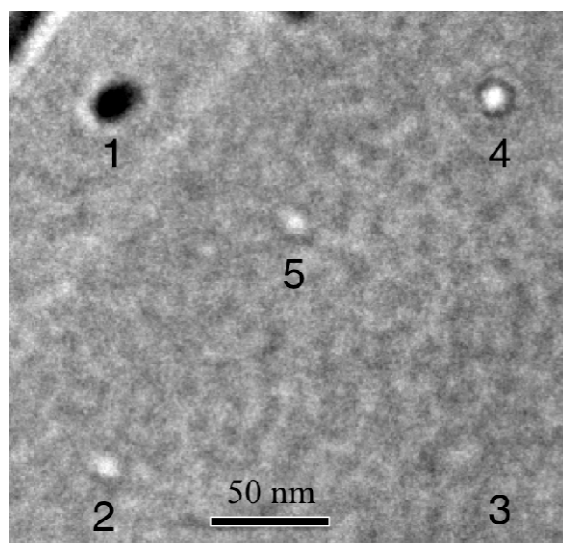


Figure S2. Depiction of contamination. Low resolution image (taken at $-40\ \mu\text{m}$ underfocus, scale bar $50\ \text{nm}$) showing the effect of a focused electron beam irradiation for 2 minutes at the following conditions 1) Room temperature (RT), 2) $400\ ^\circ\text{C}$, 3) RT, 4) $400\ ^\circ\text{C}$, and 5) $200\ ^\circ\text{C}$ for 2 minutes each. Contamination is deposited in 1, holes are created in 2, 4, and 5, and no effect is visible in 3. The image shown here was taken after the whole cycle was performed, and is the same for each point after the experiment at this point was done. Since the C contamination at 1 is still visible after preheating, it is obvious that this contamination can not be removed by specimen heating.

Fourier transforms of the images of Figure 1 of the main text

The Fourier transform analyses were made using Image J and its “Radial Profile Plot” function (P. Baggethun, <http://rsbweb.nih.gov/ij/plugins/radial-profile.html>, 2002-2009).

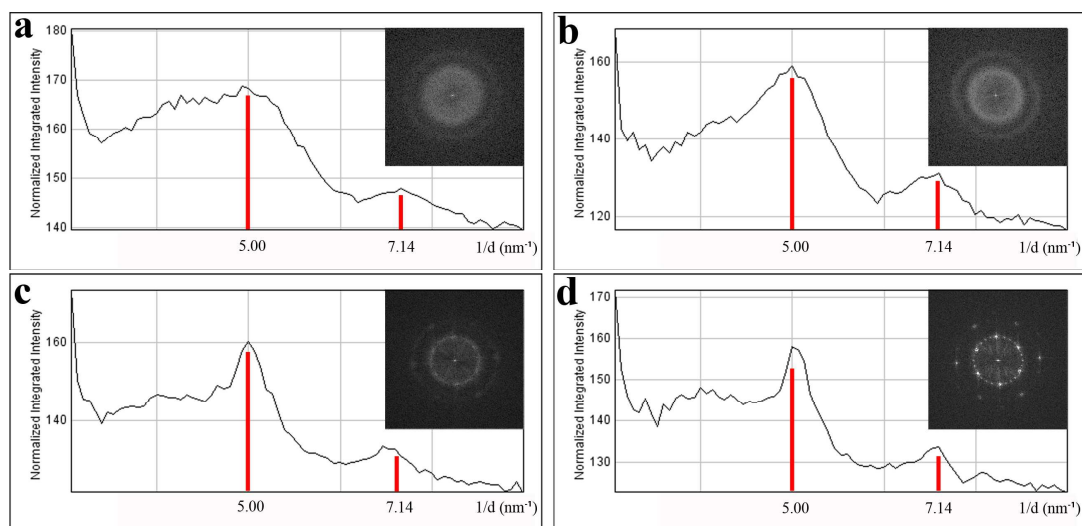


Figure S3. Rotational averages of the Fourier Transforms (FTs) of the four images in Fig. 1. The FTs are given as insets. (a) Room temperature (RT), (b) $200\ ^\circ\text{C}$, (c) $500\ ^\circ\text{C}$, and (d) $700\ ^\circ\text{C}$. The plot of RT shows an unpronounced peak at $2\ \text{\AA}$, indicating the poor absence of a long- or short-ranged ordered graphene-like structure. The plots

of 200, 500 and 700°C show an increasingly sharp peak at 2Å indicating an increasing long-range order. The FT's of 500 and 700 °C show also 100 (5 nm⁻¹) and 110 (7.14 nm⁻¹) reflections. No ring through these reflections is observed in the FT of 700°C, indicating that the graphene is single-crystalline.

Recrystallization at T>500 °C after amorphization at room temperature

An amorphous area created by e-beam exposure at room temperature can be transformed into (poly) crystalline graphene by heating to T>500 °C. A hole was made at room temperature as shown in Fig. S4a. The graphene around the hole becomes amorphous due to electron beam irradiation, which can be seen from the Fourier Transform (FT) image (Fig. S4a inset). After increasing the temperature from room temperature to 500 °C, the amorphous area around the hole is polycrystalline as shown in Fig. S4b. The FT rings (Fig. S4b inset) illustrate the polycrystalline graphene-like structure at 500 °C.

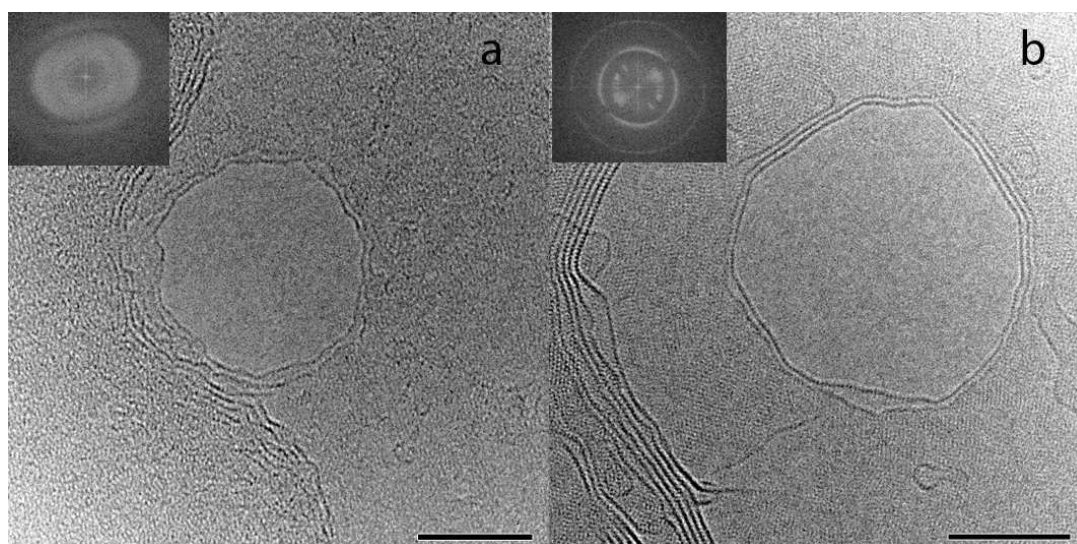


Figure S4. Recrystallisation experiments. (a) Hole made at room temperature. (b) The same area heated to 500 °C. Insets show the FTs. Scale bars are 5 nm.

Straight cylindrical nanopores

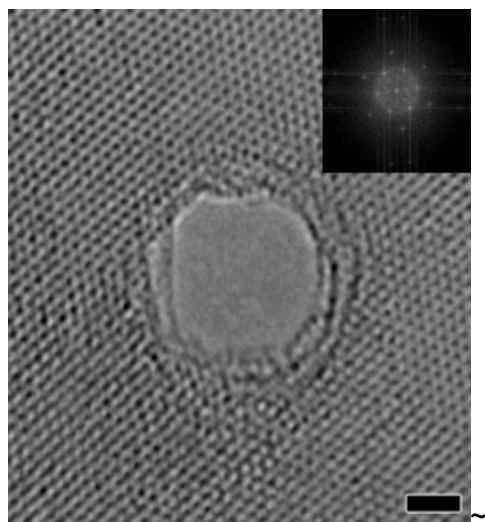


Figure S5. Straight cylindrical nanopores made at 600 °C in few-layer graphene. Scale bar, 1 nm. The FT is given as the inset.

Sculpting strategy

If one wants to make for instance an elongated hole, one can use three methods a) an elongated beam, by means of making the condenser lens astigmatic, b) a circular beam of about the width of the hole that one wants to make, which is linearly scanned, or c) a very small beam that is scanned over the intended hole area or along the circumference of the intended structure. These three modes are shown in Figure S6 as well as actual examples of the first two modes. Note that the shape of the electron beam is roughly Gaussian, which implies that the intensity falls off gradually from the centre to the tails of the beam. This implies that if the intensity in the centre of the beam is high enough to make a hole in a few seconds (by removal of all C atoms), the removal rate in the tail of the beam will be gradually less which can reduce the accuracy of the sculpting process.

Movie S3 shows a real time movie with 10 images per second of the formation of a nanopore in graphene. The electron beam is focussed on one position for 4 seconds resulting in the formation of a nanopore of $\sim 2\text{nm}$. This movie was recorded with a magnification of 580.000 times using a Flucam camera, which allows for a high recording speed and a very fast adjustment of the dynamic range, such that the focussing of the electron beam can be followed well. This camera has as disadvantage that the resolution is relatively poor, and because of that the graphene lattice is not visible. But the nanopore is well visible as soon as the beam is slightly

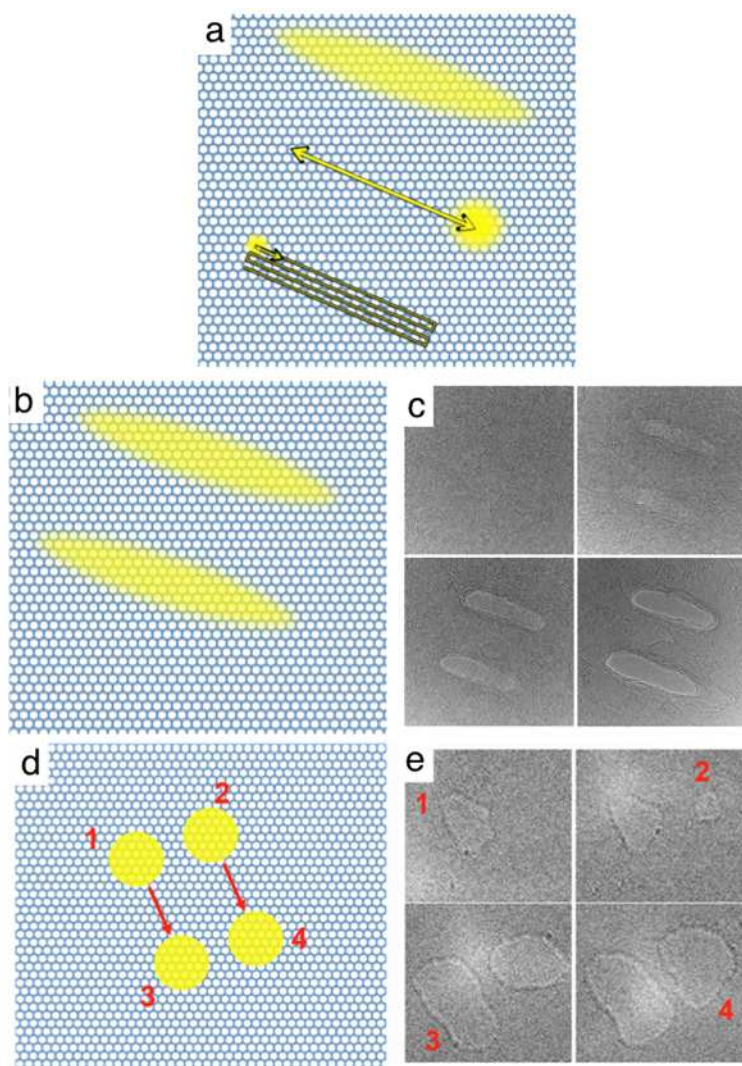


Figure S6. Sculpting strategy. (a) An elongated hole can be made with an elongated beam (made by introducing astigmatism of the condenser lens), by linearly scanning a beam of approximately the width of the hole one intends to make, or by scanning a small beam along a certain trajectory, b) shows a schematic representation of the use of an elongated beam to create a bridge. c) a sequence of images showing the actual making of such a bridge, whereby the formation of two holes is checked a few times. d) shows schematically the use of circular beams to create a bridge and e) time snapshots during the fabrication (300keV, 600 °C). The time for digging one hole in (e) is about 2~5 s.

Carbon nanotubes

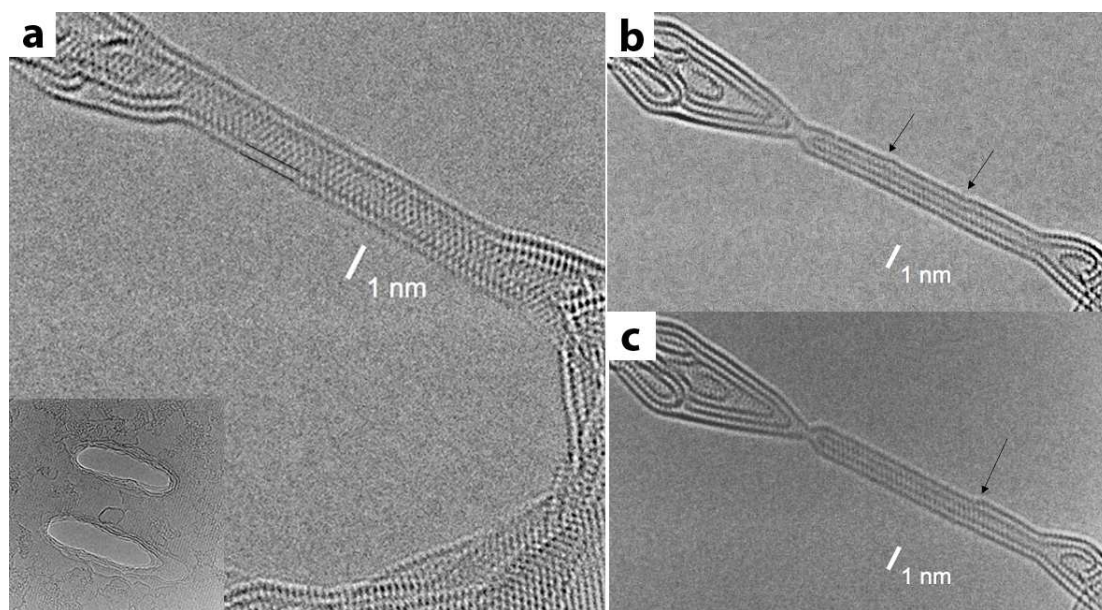


Figure S7. Carbon nanotubes made from few-layer graphene at 700 °C. (a) a carbon nanotube made using elongated electron beams with a shape similar to the holes made (inset). (b)-(c) show two frames from a movie (See Movie S4) in which the reduction in width of the CNT can be followed, finally leading a breaking of the CNT. In (a) the tube is about 1.2 nm wide. In (b) two steps in the width of the tube can be observed (indicated by arrows). The inner tube varies from 6 rings to 7 rings and 8 rings with the steps at the arrows. In (c), which is taken 5 seconds later, only a single step (indicated by arrow) in the nanotube width can be observed.

Polycrystalline graphene nanoribbon

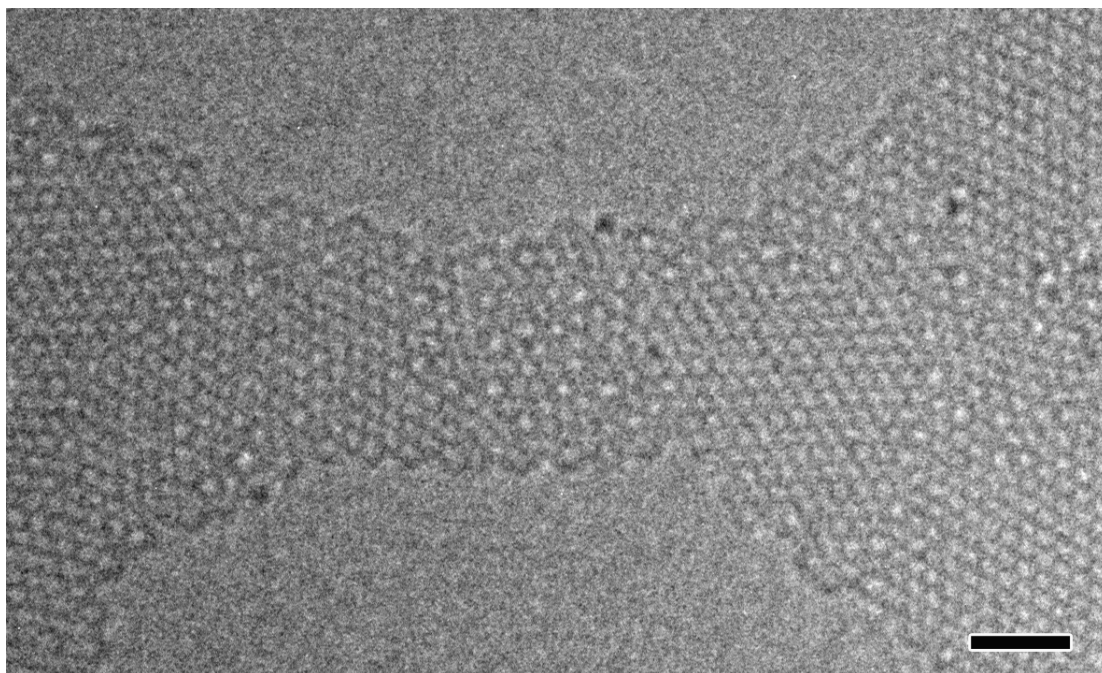


Figure S8. A polycrystalline graphene nanoribbon made at 500 °C. Ad-atoms can be seen on the edge and surface of the nanoribbon as dark dots. See Movie S6. Scale bar, 1 nm.

Prospective: More efficient sculpting of graphene by better hardware

The e-beam sculpting of graphene can be further optimized by even better hardware. The use of imaging cameras with high detection efficiency like the CMOS cameras, that now become available with allow easier imaging of the sculpted graphene without additional modifications by the electron beam. Note that due to the low contrast of the graphene, one needs to use a relatively high electron dose. The use of a high brightness gun and a probe corrector allow for a smaller high intensity beam and thus a higher precision in the sculpting. Further developments in low drift heating holders will allow longer exposure times and thus the use of less electrons per second.

Movies

Movie S1: a polycrystalline monolayer at 500 °C

Movie S2: self-repair at 600 °C

Movie S3: the sculpting process of a nanopore at 600 °C

Movie S4: carbon nanotube formation at 600 °C

Movie S5: flat tube formation at 600 °C

Movie S6: polycrystalline bridge formation at 500 °C

Movie S7: Armchair nanoribbon at 700 °C

Movie S8: single carbon chain formation at 600 °C

References

- [S1] van Huis, M. A.; Young, N. P.; Pandraud, G.; Creemer, J.F.; Vanmaekelbergh, D.; Kirkland, A. I. and Zandbergen, H. W. Atomic imaging of phase transitions and morphology transformations in nanocrystals. *Adv. Mater.* **21**, 4992–4995 (2010).
- [S2] Blake, P., Novoselov, K. S., Castro Neto, A. H., Jiang, D., Yang, R., Booth, T. J., Geim, A. K., Hill, E. W. Making graphene visible. *Appl. Phys. Lett.* **91**, 063124 (2007).
- [S3] Schneider, G. F., Calado, V. E., Zandbergen, H., Vandersypen, L. M. K. and Cees Dekker. Wedging transfer of nanostructures. *Nano Lett.* **10**, 1912 (2010).